Propagation Properties and Stress Sensitivity of S-PCF, H-PCF and O-PCF

M. R. Khatun and M. S. Islam
Institute of Information and Communication Technology
Bangladesh University of Engineering and Technology
Dhaka-1000, Bangladesh
Email: rokeya.alam@yahoo.com, mdsaifulislam@iict.buet.ac.bd

***Abstract*— Propagation properties of square, hexagonal and octagonal lattice photonic crystal fibers (PCFs) have been analyzed here for both stressed and unstressed conditions. The analysis has been carried out using finite element method. All types of PCFs are investigated here by varying number of air hole rings with same design and operating parameters. The results show that external stress causes PCFs deformation as well as change of propagation properties and this effect is not same for different types of PCFs. We have found that hexagonal PCFs are comparatively more sensitive than square and octagonal for birefringence properties. Furthermore propagation properties of octagonal PCFs remain almost unchanged with the increase of external stress. It is also found that PCFs with lower number of number of air hole rings is comparatively highly sensitive than higher number of air hole rings.**

***Index Terms*— Photonic crystal fiber, finite element method, confinement loss and elasto-optic effect.**

I. Introduction

Optical fiber communication system is a subject of growing interest due to its extremely attractive features. Photonic crystal fibers (PCFs) are one type of optical fiber. It is commonly characterized by a series of air holes that running along the fiber length [1]. PCFs are generally divided into two main categories: index guiding fibers that have a solid core and photonic band gap or air guiding fibers that have periodic micro-structured elements and a core of low index material (e.g. hollow core). PCF has ability to be single mode over a broad range of wavelengths [2]. The design of PCFs is very flexible. There are several parameters to manipulate: lattice pitch, air hole shape and diameter, refractive index of the glass, and type of lattice [3]. PCFs are of great interest for optical communication in new wavelength regions and for new optical devices. The strong wavelength dependency of the effective refractive index and the inherently large design flexibility of PCF allow for a whole new range of novel properties [4]. Such properties include endlessly single-mode fibers, extremely nonlinear fibers and fibers with anomalous dispersion in wide wavelength region. Applications of PCF includes spectroscopy, metrology, biomedicine, imaging, telecommunication, industrial machining, military and the list keeps growing as the technology becomes a mainstream [5-6].

Many experiments and investigation has been carried out using different analysis techniques and tools to understand the propagation properties of various PCFs [7-8]. Such properties include endlessly single-mode, extremely nonlinearity, highly-birefringence (hi-bi), polarization maintenance, large mode area and anomalous dispersion in visible wavelength region. These properties have been achieved by varying the design parameters of PCF. Their special properties make very attractive for a wide range of applications. In practical use it is also very important to know the properties of PCF to fully understand the feasibility of using it as sensor for stress civil structures or acoustic pressure in underwater and underground communication systems. An influence of hydrostatic pressure on phase and group modal birefringence has been theoretically analyzed in [9]. Analysis of the impact of external stress on effective index, birefringence, mode field profiles, and spot size for the two fundamental quasi-TE and TM modes has been implemented in [11]. The effect of thermal and external stress on effective index, the birefringence and PMD has been carried out on hexagonal PCF with fixed pitch and air hole diameter [12]. Strong stress dependence of birefringence and confinement loss has been shown in [13]. Here hexagonal air hole arrangement with fixed pitch and air hole diameter has been used. From previous works we see most of the works done to find the stress effect on birefringence property with hexagonal air hole arranged PCFs [10-15]. A few works has been done on confinement loss and PMD. Still the effect of external stress on effective area, effective index and confinement loss for different structured PCFs is unexplored. Mainly the properties for square, octagonal and dectagonal PCFs with external stress are unexplored. This unexplored area has motivated us to carry out this research work.

In this work, square, hexagonal and octagonal PCFs have been designed by varying their number of air hole rings. At first the propagation properties are observed here without considering external stress. Then different stress is applied on the PCFs boundary and birefringence,

Manuscript received February 15, 2011; revised May 15, 2011; accepted July 31, 2011.

doi:10.4304/jcm.7.11.832-839

confinement loss, effective area and dispersion are calculated as a function of stress. It is observed that hexagonal PCFs with lower number of air hole rings are more sensitive than others. Again with the increase of number of air hole rings it become less sensitive. But octagonal PCFs properties remain almost same with the increase of stress.

II. FORMULATION

Finite Element Method (FEM) with the perfectly matched layer (PML) boundary is used for stress and optical analysis. In the modal solution approach based on the FEM, the intricate cross section of a PCF can be represented by using many triangles of different shapes and sizes. Under external forces, the fiber is deformed and a stress distribution is formed in the fiber. Again with the application of external stress fiber deformation takes place and amount of deformation is not same for all types of PCFs. It varies depending on air filling fraction, total amount of air area and circular symmetry in fiber cross section. Fiber deformation and stress distribution in fiber cross section both causes change in fiber propagation properties. The new refractive index for x and y polarized light under external stress can be calculated from the following equations [15]

$$n_x = n_{x0} + C_1\sigma_x + C_2(\sigma_y + \sigma_z) \quad (1.1)$$

$$n_y = n_{y0} + C_1\sigma_y + C_2(\sigma_x + \sigma_z) \quad (1.2)$$

$$n_z = n_{z0} + C_1\sigma_z + C_2(\sigma_x + \sigma_y) \quad (1.3)$$

where, C_1, C_2 are the elasto-optic coefficient of the fiber or waveguide material, n_{x0} , n_{y0} and n_{z0} are the unstressed refractive indices of the material, n_x , n_y and n_z are the main diagonal elements of the anisotropic refractive index tensor, σ_x , σ_y and σ_z are the main diagonal stress vectors.

Boundary condition along the outside of the cladding the magnetic field is set to zero. For a valid boundary condition the amplitude of the field decays rapidly as a function of the radius of the cladding.

The complex effective refractive indexes of bound modes are solved from Maxwell's equations. It involves dealing with perpendicular hybrid mode waves. The mode analysis is made on a cross-section in the x-y plane of the fiber.The wave propagates in the z direction has the form

$$\mathrm{H}(x, y, z, t) = \mathrm{H}(x, y)e^{j(\omega t - \beta z)} \quad (2)$$

where, ω is the angular frequency and β the propagation constant.

The propagation constant is a function of refractive index and air filling fraction. The value of propagation constant varies with the change of external stress as well as fiber design parameters. The modified refractive index due to external stress is calculated from (1). With the variation of propagation constant propagation properties of optical fiber also changes.

Effective refractive index given by $n_{eff}=\beta/k_0$, where $k_0=2\pi/\lambda$ is the free-space wave number and λ is free space wavelength.

The modal birefringence of the fiber is obtained by $B_m = n_{eff}^x - n_{eff}^y$, where n_{eff}^x and n_{eff}^y are the effective indices in x and y direction respectively.

Chromatic dispersion (D) of the fundamental mode, given by the following equation:

$$D = -\frac{\lambda}{c}\frac{d^2 n_{eff}}{d\lambda^2} \quad (3)$$

Confinement loss of the fundamental mode, given by the following equation:

$$L = \frac{40\pi.\mathrm{Im}(n_{eff})\times 10^6}{\lambda.\ln(10)} \quad (4)$$

The second parameter concerns the value of the effective area defined by:

$$A_{eff} = \frac{(\iint |E|^2 dxdy)^2}{\iint |E|^4 dxdy} \quad (5)$$

The area integration is carried out over the cross section of the fiber and the electric field intensity E is given by,

$$E = \sqrt{E_x^2 + E_y^2} \quad (6)$$

where, E_x is the x-component of the electric field
E_y is the y-component of the electric field.

III. EXPERIMENTAL RESULT

We have considered here three types of air hole arrangements for PCFs designing.

- S-PCF (the PCF structure is designed by square shaped air hole arrangement).
- H-PCF (the PCF structure is designed by hexagonal shaped air hole arrangement).
- O-PCF (the PCF structure is designed by octagonal shaped air hole arrangement).

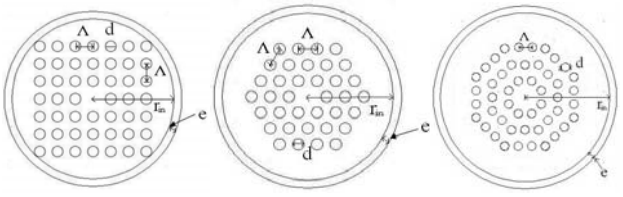

Fig. 1 Cross sections of PCFs (a) S_PCF (b) H-PCF (c) O-PCF, where d=1.4μm, Λ=2.3μm, e=1μm, r_{in}=12.0μm and Nr=3.

Here solid core index guiding PCFs are made by only single material (SiO2), where refractive index n_s=1.45. The number of air hole rings Nr varies from 1 to 3. For all types of PCFs some other design parameters: fiber cross sectional diameter r_{in}=12.0μm; the air hole diameter d=1.4μm; the spacing between holes or pitch Λ=2.3μm; PML thickness e=1μm is considered fixed. Fig. 1 shows the cross section of S-PCF, H-PCF and O-PCF for Nr=3. Similarly we also designed PCFs with Nr=1 and 2 with square, hexagonal and octagonal air hole arrangements.

A. Air Filling Fraction

Air filling fraction (AFF) of PCF is the ratio of total area of air in fiber cross section to total cross sectional area of the fiber. It presents the amount of air in the fiber cross section.

$$AFF = \frac{A_{hole}}{A_{cell}} \tag{7}$$

where,
A_{hole}= area of the air hole inside the unit triangle,
A_{cell}= area of the unit triangle.

Fig.2 (a), (b) and (c) show the unit triangles for S-PCF, H-PCF and O-PCF respectively.

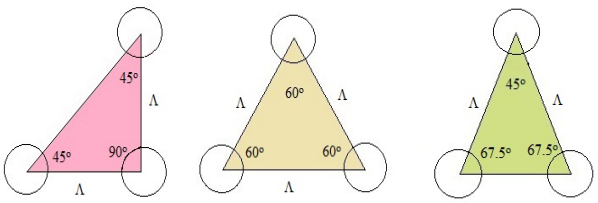

Fig.2 The unit triangle (a) S-PCF, (b) H-PCF, (c) O-PCF.

Area of a circular air hole, $a_{hole} = \pi r^2 = \pi \frac{d^2}{4}$ (8)

where, r is the radius of the air hole.

The unit triangle has ½ area of an air hole. Because, it covers 180° area of a circular air hole.
So area of air hole in a triangle,

$$A_{hole} = \frac{a_{hole}}{2} = \pi \frac{d^2}{2 \times 4} = \pi \frac{d^2}{8} \tag{9}$$

From the figure we can see that the unit triangle for S-PCF is a right triangle. We get the area of unit triangle for S-PCF according to the rules of right angle. $A_{cell(Sqr)} = \frac{1}{2}\Lambda^2$.

∴ Air filling fraction for S-PCF is

$$AFF_{Sqr} = \frac{\frac{\pi d^2}{8}}{\frac{1}{2}\Lambda^2} = \frac{\pi}{4} \times \left(\frac{d}{\Lambda}\right)^2 \tag{10}$$

We get the area of unit triangle for H-PCF,

$$A_{cell(Hexa)} = \frac{1}{2}\Lambda^2 \times Sin(60^o) = \frac{\sqrt{3}}{4}\Lambda^2 \tag{11}$$

∴ Air filling fraction for H-PCF is

$$AFF_{Hexa} = \frac{\frac{\pi d^2}{8}}{\frac{\sqrt{3}}{4}\Lambda^2} = \frac{\pi}{2\sqrt{3}} \times \left(\frac{d}{\Lambda}\right)^2 \tag{12}$$

Similarly we get the area of unit triangle for O-PCF,

$$A_{cell(Octa)} = \frac{1}{2}\Lambda^2 \times Sin(45^o) = \frac{1}{2\sqrt{2}}\Lambda^2 \tag{13}$$

∴ Air filling fraction for O-PCF is

$$AFF_{Octa} = \frac{\frac{\pi d^2}{8}}{\frac{1}{2\sqrt{2}}\Lambda^2} = \frac{\pi}{2\sqrt{2}} \times \left(\frac{d}{\Lambda}\right)^2 \tag{14}$$

From the above equations (10), (12) and (14) we find that

$$AFF_{Sqr} \angle AFF_{Hexa} \angle AFF_{Octa}$$

Again, total number of air holes in symmetrically arranged PCF is

$$N = \sum_{i=0}^{Nr} i \times n_r = \frac{1}{2} Nr \times (Nr+1) \times n_r \tag{15}$$

where, n_r=8, 6 and 8 for S-PCF, H-PCF and O-PCF respectively.

Again we have considered here only circular shape air holes and area of each air hole is πr^2. Under same number of air hole rings and air hole diameter A_s, A_h and A_o are the total air-hole cross sectional area for S-PCF, H-PCF and O-PCF respectively. By mathematical calculation it is found that $A_0 = 1.33A_h$ and $As = 1.33A_h$. That means total air-hole cross sectional area for S-PCF and O-PCF is about 33% greater than H-PCF with same Nr and d. From the experimental results it is found that H-PCFs are comparatively more sensitive than S-PCFs and O-PCFs for birefringence property. It infers that PCFs with smaller air area are more sensitive than the PCFs with larger air area for this property.

To find out the external stress effect on fiber structure and propagation properties the analysis has been carried out using COMSOL Multiphysics FEMLAB modeling and simulation tool. The mode analysis has been made on a cross-section in the x-y plane of the fiber. We have considered here both stressed and unstressed PCFs to understand the effect of stress on fiber propagation properties. To understand the effects of stress on the fibers at first 1GP and then 5GPa uniform external stress have been applied on fibers boundary from all directions, where operating wave length varied from 1μm to 2μm.

B. Maximum Displacement

External stress causes fiber deformation in all direction. So that it causes fiber structural changes as well as propagation properties. Here we have observed maximum displacement to measure amount of maximum deformation in fiber cross section due to external stress. Furthermore external stress induced displacement is not same for different types of PCFs.

Fig.3 shows maximum displacement as a function of stress for S-PCFs, H-PCFs and O-PCFs. From the figure it is clear that with the increase of external stress displacement also increases and it is high for larger number of air hole rings. From the mathematical analysis we get total air area in fiber cross section is comparatively higher for S-PCF and O-PCF than H-PCF. Again, from simulation result we get maximum displacement also high for S-PCF and O-PCF than H-PCF.

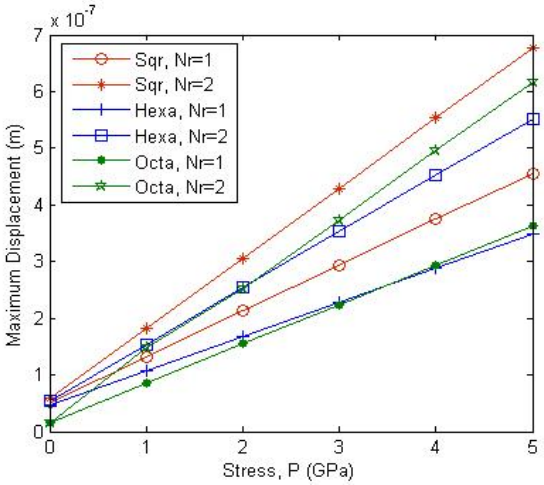

Fig. 3 Maximum displacement as a function of external stress and number of air rings for S-PCF, H-PCF and O.PCF.

C. Effective Index

The effective index is found as the modal solution of optical analysis. Fig. 4 shows the combined results of effective index as a function of wavelength for all types of unstressed PCFs with Nr=1 and 3. It depicts that without any external stress effective index gradually decreases with the increase of wavelength. It also shows that effective index of O-PCF is less than both S-PCF and H-PCF and it is always greater for S-PCFs than H-PCF. External stress acting on the PCFs makes change in fiber material refractive index. To get the stress effect on effective index at first we carried out stress analysis then optical.

Fig. 5 shows the variation of effective index as a function of wavelength under external stress. For stressed PCFs refractive index also decreases with the increase of wavelength and with the increase of external stress effective index increases for all types of PCFs that agrees with the result found in [11]. But this change is comparatively more for S-PCF and H-PCF than O-PCF.

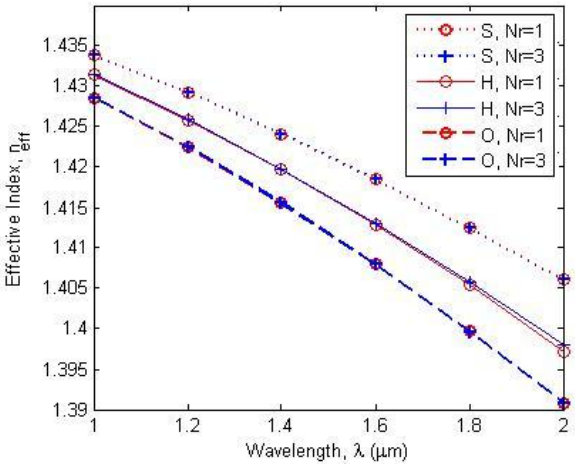

Fig. 4 Effective index as a function of wavelength for unstressed PCFs with different number of air hole rings, where d=1.4μm, Λ=2.3μm and r_{in}=12.0μm.

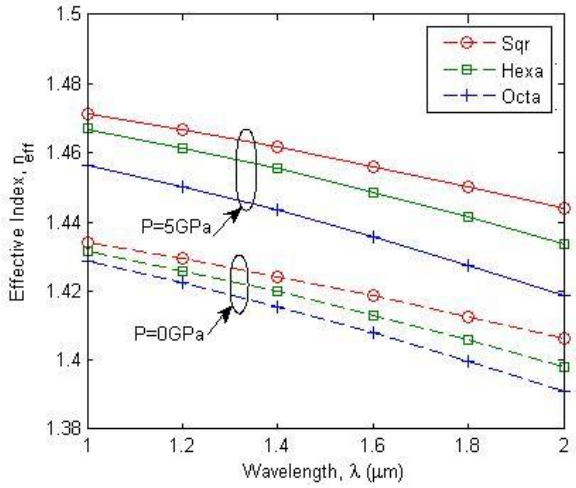

Fig. 5 Effective index as a function of wavelength and stress for S-PCF, H-PCF and O-PCF, where d=1.4μm, Λ=2.3μm, Nr=3 and r_{in}=12.0μm.

D. Birefringence

External stress on PCF causes stress distribution and fiber deformation in fiber cross section. This deformation is not same for all types of fiber and in all direction (x and y), which causes different birefringence for different types of PCFs. For unstressed PCFs birefringence is very small for all types of fibers. But considering external stress it increases with the increase of stress that agrees with the result found in [11]. Fig. 6, Fig. 7 and Fig. 8 depict the variation of birefringence as a function of wavelength for S-PCFs, H-PCFs and O-PCFs respectively. We can see here that birefringence increases with the increase of wavelength and stress for all types of fibers and the change is more for lower number of air hole rings with larger operating wavelength. It is also found that external stress induced birefringence is higher (order of 10^{-4}) for H-PCFs than S-PCF and O-PCF with whole operating wavelengths (1μm to 2μm).

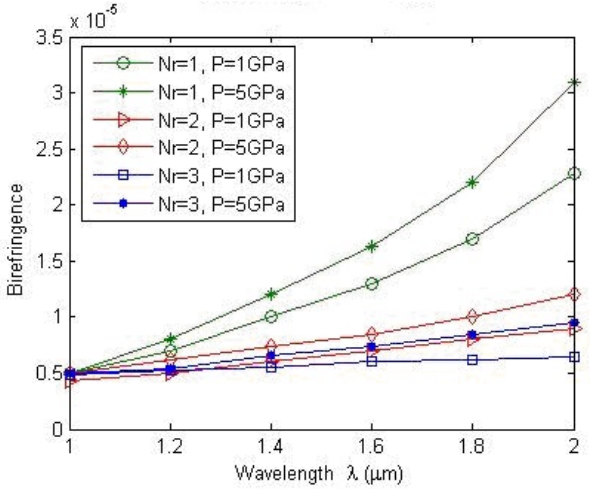

Fig. 6 Birefringence as a function of wavelength and external stress for S-PCFs with different number of air hole rings, where d=1.4μm, Λ=2.3μm and r_{in}=12.0μm.

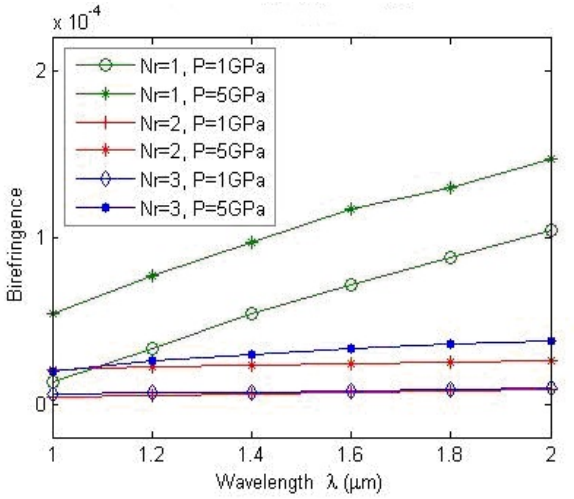

Fig. 7 Birefringence as a function of wavelength and external stress for H-PCFs with different number of air hole rings, where d=1.4μm, Λ=2.3μm and r_{in}=12.0μm.

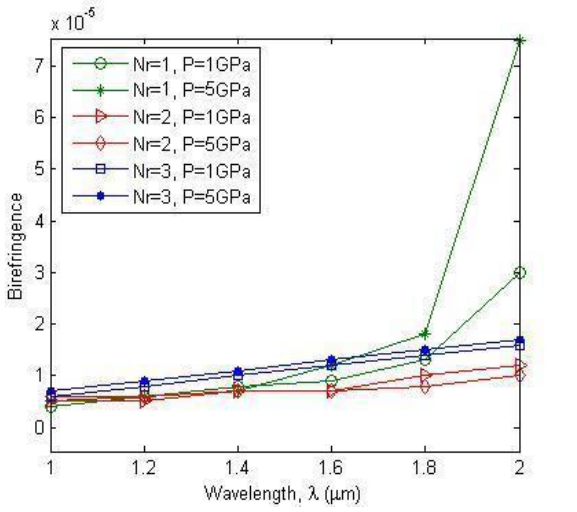

Fig. 8 Birefringence as a function of wavelength and external stress for O-PCFs with different number of air hole rings, where d=1.4μm, Λ=2.3μm and r_{in}=12.0μm.

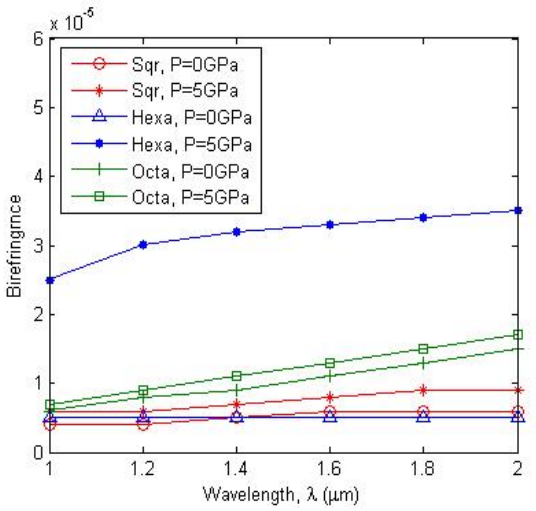

Fig.9 Birefringence as a function of wavelength and external stress for S-PCF, H-PCF and O-PCF, where d=1.4μm, Λ=2.3μm and Nr=3.

Fig. 9 depicts that without considering external stress birefringence is almost same (order of 10^{-6}) for S-PCF and H-PCFs and it is more for O-PCF. In this case we have considered that PCFs are designed with Nr=3. Furthermore with 5GPa external stress birefringence increases very sharply (order of 10^{-4}) for H-PCF but this change is very low for S-PCF and O-PCF. Again birefringence for O-PCF with 5GPa external stress is comparatively higher than S-PCF.

E. Confinement Loss

External stress causes increase of confinement loss for all types of PCFs. The following figures Fig. 10, Fig. 11 and Fig. 12 show combined (S-PCF, H-PCF and O-PCFs) results of confinement loss as a function of wavelength and stress, where d=1.4μm and Λ=2.3μm. Fig. 10, Fig. 11 and Fig. 12 show the results for the PCFs with Nr=1, Nr=2 and Nr=3 respectively. All the mentioned figures depict that confinement loss increases with the increase of wavelength for all types of PCFs that agrees with the result found in [12]. It is always higher for H-PCFs than S-PCF and O-PCF, where PCFs are designed with Nr=1 and 2. Again S-PCF shows comparatively higher confinement loss than O-PCF. It is also noticeable that external stress induced confinement loss is very high for both S-PCF and H-PCFs with Nr=1. Confinement loss decreases with the increase of number of air hole rings and it changes more sharply for H-PCFs than others. But S-PCFs with Nr=3 shows high stress sensitivity than H-PCF and O-PCF. At this case O-PCFs show that confinement loss remains very low and almost unchanged with the increase of stress. Again Fig. 13 shows confinement loss as a function of wavelength in x-axis and y-axis for all types of PCFs, where d=1.4μm, Λ=2.3μm, e=1μm, r_{in}=12.0μm, Nr=3 and P=5GPa. This figure shows that external stress induced confinement loss is higher in y-axis than x-axis. S-PCF shows large difference between x-axis and y-axis confinement loss than other types of PCFs with the increase of external stress.

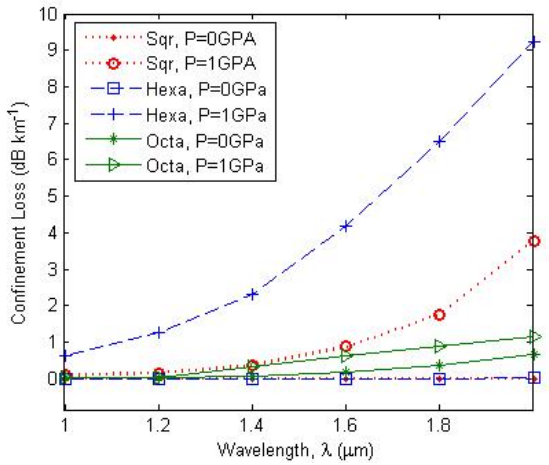

Fig. 10 Confinement loss as function of wavelength and external stress for S-PCF, H-PCF and O-PCF, where d=1.4μm, Λ=2.3μm, e=1μm, r_{in}=12.0μm and Nr=1.

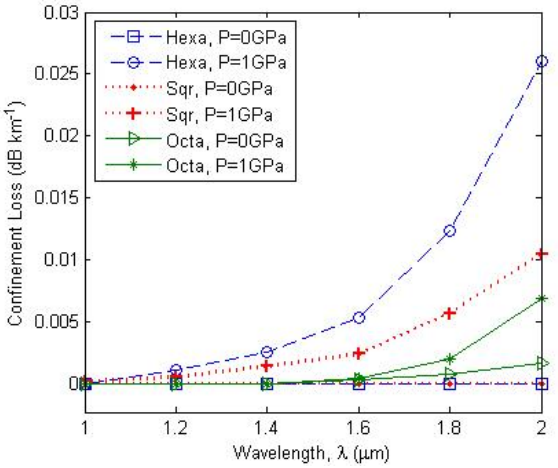

Fig. 11 Confinement loss as a function of wavelength and external stress for S-PCF, H-PCF and O-PCF, where d=1.4μm, Λ=2.3μm, e=1μm, r_{in}=12.0μm and Nr=2.

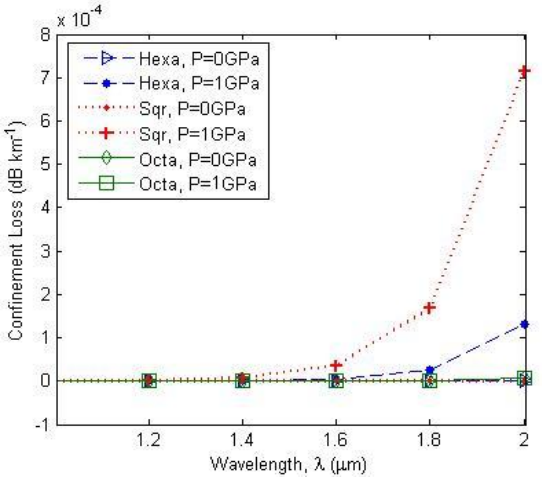

Fig. 12 Confinement loss as a function of wavelength and external stress for S-PCF, H-PCF and O-PCF, where d=1.4μm, Λ=2.3μm, e=1μm, r_{in}=12.0μm, Nr=3.

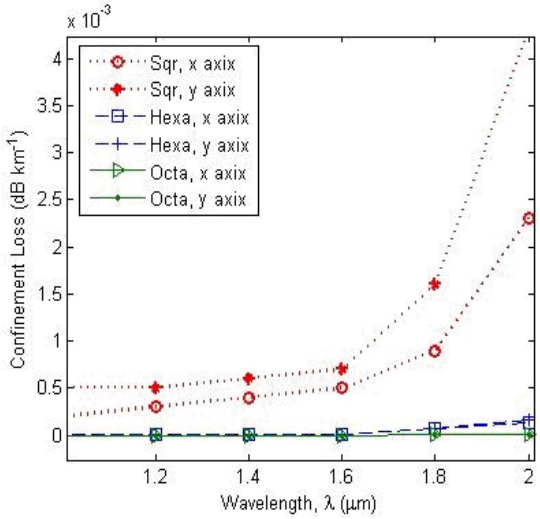

Fig. 13 Confinement loss as a function of wavelength in x-axis and y-axis for S-PCF, H-PCF and O-PCF, where d=1.4μm, Λ=2.3μm, e=1μm, r_{in}=12.0μm, Nr=3 and P=5GPa.

F. Effective Area

Fig. 14 shows that without considering external stress effective area increases with the increase of wavelength for all structures. It also shows that effective area of square shape PCFs are always greater than hexagonal and octagonal shape. Furthermore it shows that with the increase of Nr it decreases for all types of PCFs. Fig. 15 shows effective area as a function of wavelength and external stress for H-PCFs and O-PCFs, where d=1.4μm, Λ=2.3μm and Nr=3. This figure shows that effective area slowly increases with the increases of wavelength and it is always higher for S-PCFs than H-PCFs and O-PCFs. It also shows 5GPa external stress induces higher effective area with shorter wavelength than longer. But external stress induced change of effective area is very small for O-PCFs.

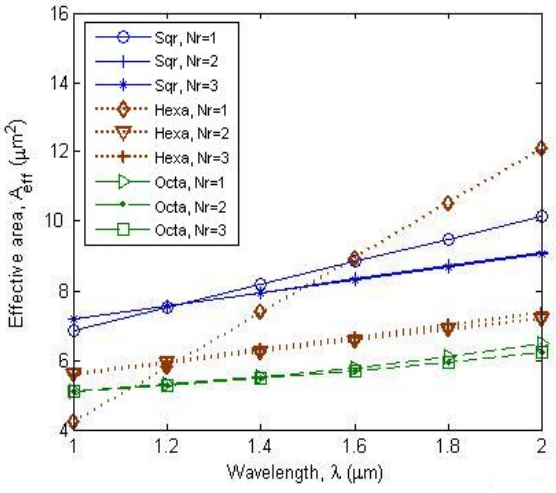

Fig. 14 Without considering external stress effective area as a function of wavelength for S-PCFs, H-PCFs and O-PCFs, where d=1.4μm, Λ=2.3μm and Nr=3.

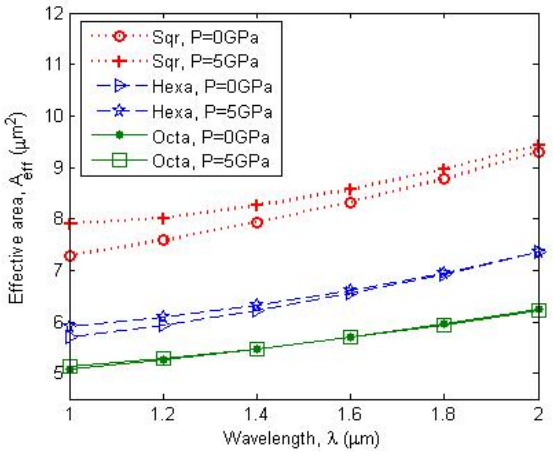

Fig. 15 Effective area as a function of wavelength and external stress for S-PCF, H-PCF and O-PCF, where d=1.4μm, Λ=2.3μm and Nr=3.

G. Dispersion

Dispersion as a function of wavelength and number of air hole rings for unstressed S-PCF, H-PCF and O-PCF have been shown in Fig. 16, where d=1.4μm, Λ=2.3μm and P=0GPa. From this figure we can see that dispersion is always higher for O-PCF than S-PCF and H-PCF. Again it is higher for H-PCF than S-PCF. We also find that dispersion for all types of PCFs increases with the increase of wavelength and PCFs with higher number of air hole rings show higher dispersion.

Furthermore Fig. 17 shows dispersion as a function of wavelength only for H-PCFs. Here we have designed PCFs by varying Nr=1, 2 and 3 and external stress have been applied as 0GPa, 1GPa and 5GPa. It also shows that external stress causes increase of dispersion and this effect is low for the PCFs with higher Nr.

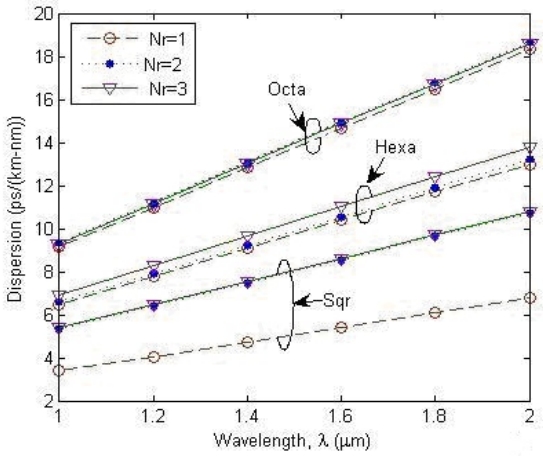

Fig. 16 Without considering external stress dispersion as a function of wavelength for S-PCFs, H-PCFs and O-PCFs, where Nr=1, 2 and 3.

Fig. 18 shows dispersion as a function of wavelength and external stress for S-PCF, H-PCF and O-PCF, where all design and operating parameters are same (d=1.4μm, Λ=2.3μm and Nr=3). To compare the stress effect on the PCFs we have considered here P=0GPa (unstressed) 1GPa and 5GPa external stress. From the figure we can find that dispersion for O-PCF is higher than H-PCF and S-PCF. Again H-PCF shows higher dispersion than S-PCF. With 5GPa external stress all types of PCFs show higher dispersion than 0GPa.

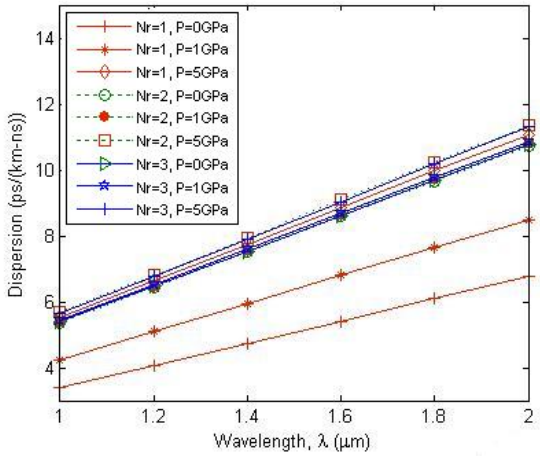

Fig. 17 Considering external stress dispersion as a function of wavelength, number of air hole rings and external stress for H-PCFs.

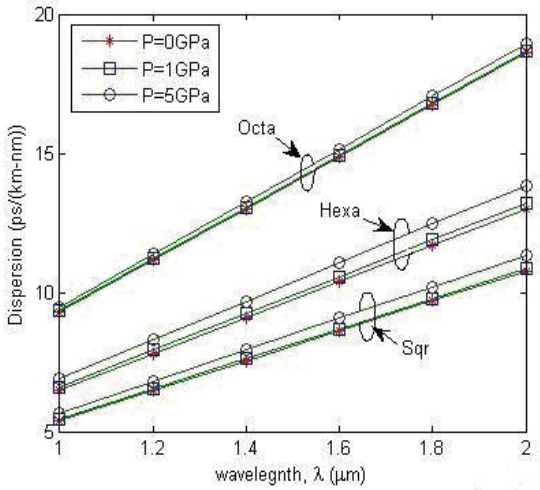

Fig. 18 Dispersion as a function of wavelength and external stress for S-PCF, H-PCF and O-PCF, where d=1.4μm, Λ=2.3μm and Nr=3.

H. Comparison with Related Published Works

In Ref. [10], [12] and [13] the authors have observed stress sensitivity of H-PCF with different air hole diameter. They have showed that birefringence increases with the increase of external stress. In our research work we have considered S-PCF, H-PCF and O-PCF with different number of air hole rings and air hole diameter. We have found that with the increase of external stress birefringence increases almost linearly for all types of PCFs and this change is always higher for hexagonal than square and octagonal. At external stress 5GPa, hexagonal, octagonal and square PCFs show birefringence of order of 10^{-4}, 10^{-5} and 10^{-6} respectively.

Lateral stress induced confinement loss for hexagonal PCFs with fixed pitch and the air hole diameter have been observed in [13]. Where the results of simulation show us strong stress dependency of confinement loss and it increases with the increase of external stress. At 1.6 μm

wavelength force 1.5GPa causes confinement loss around order of 10^{-3} (dB/Km). In our research work we have analyzed the effect of external stress for square, hexagonal and octagonal PCFs with different number of air hole rings and air hole diameter. We have also found that confinement loss increases with the increase of stress and this change is very sharp for longer wavelength and this change is always higher for hexagonal PCFs than square and octagonal. PCFs with larger air hole diameter and higher number of air hole rings show lower confinement loss. With pitch 2.3μm air hole diameter 1.4μm, S-PCF, H-PCF and O-PCF with external stress 1.5GPa show confinement loss of order of 10^{-4}, 10^{-5} and 10^{-7} respectively.

IV. Conclusion

In this research work, analysis has been carried out to observe the effect of external stress on propagation properties of square, hexagonal and octagonal air hole arranged PCFs. Here we have designed the PCFs by varying only number of air hole rings. We have considered here both stressed and unstressed PCFs to understand the effect of stress on the propagation properties. From the results it have been found that with same design parameters S-PCF shows larger effective area and low dispersion than others. H-PCFs show high birefringence, high confinement loss and low dispersion. Again O-PCF shows very low birefringence and dispersion. Under external stress with different number of air hole rings S-PCF and H-PCF is comparatively more sensitive than O-PCF. There are many applications of PCFs and depending on these types of application specific properties of PCFs get importance. Our finding will help to select the appropriate designing of PCF for some of particular application.

References

[1] K. Saitoh and M. Koshiba, "Numerical modeling of photonic crystal fibers", Journal of Lightwave Technology, vol. 23, no. 11, pp. 3580 – 3590, 2005.

[2] J. S. Chiang and T. L. Wu, "Analysis of propagation characteristics for an octagonal photonic crystal fiber (O-PCF)", Optics Communications Journal, vol. 258, no. 2, pp. 170–176, 2006.

[3] L. Zhao-Lun, L. Lan-Tian and W. Wei, "Tailoring nonlinearity and dispersion of photonic crystal fibers using hybrid cladding", Brazilian Journal of Physics, vol. 39, no. 1, pp. 50-54, 2009.

[4] M. M. Roja and R. K. Shevgaonkar, "Geometrical Parameters Identification for Zero Dispersion in Square Lattice Photonic Crystal Fiber using Contour Plots", IEEE Proceedings, Signal processing, Communications and Networking, pp. 116 – 118, 2008.

[5] M. Pourmahyabadi and S. M. Nejad, "Numerical analysis of index-guiding photonic crystal fibers with low confinement loss and ultra-flattened dispersion by FDFD method", Iranian Journal of Electrical & Electronic Engineering, vol. 5, no. 3, pp.170-197, 2009.

[6] S. S. A. Obayya, B. M. A. Rahman and K. T. V. Grattan, "Accurate finite element modal solution of photonic crystal fibers," lEEE Proceedings, Optoelectronics, vol. 152, no. 5, pp. 241-246, 2005.

[7] N. A. Mortensen, "Effective area of photonic crystal fibers", Optic Express, vol. 10, no. 7, pp. 314-348, 2002.

[8] W. C. Chew and W. H. Weedon, "A 3D perfectly matched medium from modified Maxwell's equations with stretched coordinates," IEEE Photonic Technology Letter, vol. 7, no. 13, pp. 599-604, 1994.

[9] M. Szpulak, T. Martynkien and W. Urbanczyk, "Effects of hydrostatic pressure on phase and group modal birefringence in micro-structured holey fibers", Applied Optics Journal, vol. 43, no. 24, pp. 4739-4744, 2004.

[10] M. S. Alam, N. Somasiri, B. M. A. Rahman and K. T. V. Grattan, "Effects of High External Pressure on Photonic Crystal Fiber," Proceedings of the Third International Conference on Electrical and Computer Engineering, ICECE, pp. 245-248, 2004.

[11] M. A. Hossain and M. S. Alam, "Polarization properties of photonic crystal fibers considering thermal and external stress effects", Proceedings of International Conference on Advanced Communication Technology, ISSN. 1738-9445, pp. 879 – 883, 2010.

[12] H. Tian, Z. Yu, Han L. and Y. Liu, "Birefringence and confinement loss properties in photonic crystal fibers under lateral stress", IEEE Photonic Technology. Letter, vol. 20, no. 22, pp.1830-1831, 2008.

[13] Z. Zhu and T. G. Brown, "Stress-induced birefringence in micro structured optical fibers", Optical Letters, vol. 28, no. 23, pp. 495 – 503, 2003.

[14] W. J. Bock, J. Chen, T. Eftimov, and W. Urbanczyk, "A photonic crystal fiber sensor for pressure measurements", IEEE Proceedings, Transactions on Instrumentation and Measurement, vol. 55, no. 4, pp. 1119–1123, 2006.

[15] K. Okamoto, T. Hosaka and T. Edahiro, "Stress analysis of optical fibers by a finite element method," IEEE Journal. Quantum Electronics, QE-17, pp. 2123-2129, 1981.

M. R. Khatun was born in Chuadanga, Bangladesh. She obtained B.Sc. Eng. degree in Computer Science and Engineering in 2005 from Khulna University of Engineering and Technology (KUET). She currently is pursuing M.Sc. Eng. degree in Information and Communication Technology from Bangladesh University of Engineering and Technology (BUET).

She is working as a lecturer in the Department of Computer Science and Engineering of International Islamic University Chittagong (IIUC). Her current research interests include optical fiber, photonic crystal fiber, wireless network and cognitive network. She has published 4 research papers in International Conferences.

M. S. Islam obtained Ph.D. from Bangladesh University of Engineering and Technology (BUET), Dhaka, Bangladesh in 2008, M. Sc in Computer Science and Engineering from Shanghai University, China in 1997 and B.Sc. in Electrical and Electronic Engineering from BUET in 1989.

He has published many research papers in national and international journals and conferences. Currently, he is working as and Professor in the institute of Information and Communication Technology (IICT) of BUET. His research interests include DWDM transmission system, dispersion, nonlinearity and wireless communication.